

FREQUENCY STRUCTURE OF MICROPULSES FROM PULSAR PSR 0950+08

J. M. CORDES

Department of Physics and Astronomy, University of Massachusetts

AND

T. H. HANKINS

National Astronomy and Ionosphere Center

Received 1978 July 14; accepted 1979 May 10

ABSTRACT

Radio-frequency spectra of short-time-scale structure (micropulses) were analyzed over a 1.25 MHz bandwidth. An autocorrelation analysis of the spectra revealed no significant frequency structure other than that expected from micropulses that are envelopes of a white Gaussian random process. This implies that there were no spectral lines or other deviations from flat spectra, that unresolved micropulses contribute negligibly to the spectra, and that a single micropulse is due to the incoherent addition of radiation from many coherently radiation emitters. The radiation bandwidth of each emitter must be at least 5 kHz and may be as large as several hundred MHz. Micropulses are probably determined by processes that are distinct from those responsible for the coherence of the radiation.

Subject heading: pulsars

I. INTRODUCTION

Single pulses from pulsars show structure with time scales from milliseconds to microseconds (Hankins 1972; Cordes and Hankins 1977; Hankins and Boriakoff 1978). In a series of papers we have analyzed pulse structure statistically and found that it is—to a good approximation—describable as an amplitude modulation of Gaussian noise. This description has been quantitatively verified (Cordes 1976*a*; Hankins and Boriakoff 1978) by analyzing the moments of pulsar signals in the time domain. A complementary test of the amplitude-modulated noise (AMN) model (Rickett 1975) involves a study of frequency-domain moments. Rickett, Hankins, and Cordes (1975) argued that the frequency structure they observed from PSR 0950+08 was qualitatively consistent with AMN. In the present paper, we make a *quantitative* comparison of the AMN model with the spectra of short-time-scale structure over a bandwidth that is 10 times that considered in the study of Rickett *et al.*, thus affording a stronger test.

In the following, we describe the AMN model, and then compare it to the data by calculating autocorrelation functions of the radio-frequency spectra of individual micropulses. We discuss the implications of our measurements, which include limits on the radiation bandwidth of individual emitters.

II. DATA ACQUISITION

Data were recorded in 1976 May at Arecibo Observatory using the 305 m antenna and the 430 MHz line feed. The signal from the (nominal) left-hand

circularly polarized port was passed through a 1.25 MHz intermediate-frequency bandpass filter. After being mixed to baseband, the undetected signal (i.e., the complex voltage which is proportional to the incident electric field) was sampled at 0.8 μ s intervals in a 26.2 ms window and recorded on magnetic tape. A hardware innovation enabled us to improve the time resolution by an order of magnitude over observing sessions reported earlier (Hankins 1972; Rickett, Hankins, and Cordes 1975; Cordes 1976*a*; Cordes and Hankins 1977). As before, the smearing due to interstellar dispersion was removed by convolving the data with a digital filter (Hankins and Rickett 1975). Filtered data were recorded in undetected form for subsequent processing.

III. FREQUENCY STRUCTURE OF MICROPULSES

In this section we first outline a statistical model from which we derive the autocorrelation function (ACF) of the spectrum. We discuss errors in estimating the autocorrelation function from data. Data are then presented which are compared with the model.

a) The Amplitude-Modulated Noise Model

In general we can write the narrow-band electric field as the sum of a pulsar (p) signal and an off-pulse noise (n) signal:

$$e(t) = p(t) + n(t). \quad (1)$$

The narrow-band signals are, by virtue of the data-taking procedure, complex quantities. The statistics of

the off-pulse noise are

$$\langle n(t) \rangle = \langle n(t)n(t + \tau) \rangle = 0, \quad (2)$$

$$\langle n(t)n^*(t + \tau) \rangle = \sigma_n^2 R_h(\tau), \quad (3)$$

$$\begin{aligned} \langle n(t_1)n^*(t_2)n(t_3)n^*(t_4) \rangle \\ = \sigma_n^4 [R_h(t_1 - t_2)R_h(t_3 - t_4) \\ + R_h(t_1 - t_4)R_h(t_3 - t_2)]. \quad (4) \end{aligned}$$

Angular brackets denote average over an ensemble, the asterisk denotes a complex conjugate, and $R_h(t)$ is the autocorrelation of $h(t)$, the baseband impulse response of the receiver. The autocorrelation $R_h(t)$ has a width equal to the inverse bandwidth, or about $0.8 \mu\text{s}$. The assumption of Gaussian statistics is embodied in equation (4), which gives the 4th moment of $n(t)$ as $2\sigma_n^4$. This is identical to the 4th moment of a complex Gaussian random variable whose real and imaginary parts are real, independent, zero-mean random variables.

The pulsar signal we write in the form

$$p(t) = a(t)m(t), \quad (5)$$

where $a(t)$ is the amplitude modulation of random noise $m(t)$. Micropulses are described by $a(t)$ while we assume that $m(t)$ has moments that are of the same form as those for $n(t)$ in equations (2)–(4); that is, $m(t)$ is also complex Gaussian noise.

The radio-frequency spectrum of $\epsilon(t)$ is the squared modulus of its Fourier transform, $\tilde{\epsilon}(\nu)$:

$$S(\nu) \equiv |\tilde{\epsilon}(\nu)|^2, \quad (6)$$

where $S(\nu)$ is, of course, a random process whose moments are determined by those of $\epsilon(t)$. The statistic most useful to us is the ACF of $S(\nu)$,

$$R_s(\delta\nu) \equiv \left\langle \int d\nu S(\nu)S(\nu + \delta\nu) \right\rangle. \quad (7)$$

Under the above-mentioned assumptions concerning the statistics of $n(t)$ and $m(t)$, and also assuming that $a(t)$ fluctuates much more slowly than do $m(t)$ and $n(t)$, $R_s(\delta\nu)$ can be written in normalized form as

$$\begin{aligned} r_s(\delta\nu) \equiv R_s(\delta\nu)/R_s(0) \\ = [m_\nu^2 \Delta(\delta\nu) + r_H(\delta\nu)] / (1 + m_\nu^2). \quad (8) \end{aligned}$$

Here $r_H(\delta\nu)$ is the normalized ACF of the receiver bandpass, $H(\nu) \equiv |\tilde{h}(\nu)|^2$, where $\tilde{h}(\nu)$ is the Fourier transform of $h(t)$. Thus $r_H(\delta\nu)$ has a width that is comparable to 1.25 MHz, the receiver bandwidth. Superposed with $r_H(\delta\nu)$ is a "spike," $\Delta(\delta\nu)$, that is nonzero only for small frequency lags and is defined as

$$\Delta(\delta\nu) = \frac{\langle |\sigma_m^2 \tilde{A}(\delta\nu) + \sigma_n^2 \sin(\pi\delta\nu T) / \pi\delta\nu T|^2 \rangle}{\langle [\sigma_m^2 \tilde{A}(0) + \sigma_n^2]^2 \rangle}, \quad (9)$$

where $\tilde{A}(\delta\nu)$ is the Fourier transform of $a^2(t)$ and T is the length of the data window. When $n(t)$ and $m(t)$

have Gaussian statistics, the modulation index m_ν is unity. Hence spike amplitudes of 0.5 are consistent with $n(t)$ and $m(t)$ being complex Gaussian random processes. The pulsar signal makes a contribution to the on-pulse ACF that is larger than the off-pulse noise contribution by a factor equal to the square of the signal-to-noise ratio. The signal-to-noise ratio is ~ 10 for the data discussed here, implying that the on-pulse ACF indeed reflects the properties of the pulsar signal.

Estimation errors of the ACFs can be calculated from the amplitude-modulated noise model. When N_i independent spectral values are used to compute the ACF, the estimation error is

$$\sigma_r(\delta\nu) \approx (1 + m_\nu^2) N_i^{-1/2} r_s(\delta\nu), \quad (10)$$

where m_ν^2 is the modulation index of the square of the pulsed intensity. The average ACF is dominated by pulses with the strongest intensity, and estimation errors are therefore larger than for a steady ($m_\nu^2 = 0$) source.

Two propagation effects in the interstellar medium, scattering and Faraday rotation, impose frequency structure on the pulsar signal that can alter the statistics of the signal. The diffraction-induced frequency structure caused by interstellar scattering has a characteristic bandwidth that scales roughly as $\nu^{4.4}$ and varies with dispersion measure as DM^{-4} (Rickett 1977). For PSR 0950+08 at 430 MHz, the characteristic bandwidth is probably several times greater than 1.25 MHz (Sutton 1971). Therefore, the spectra described below are at most only slightly modulated by scattering effects.

Faraday rotation in both the interstellar medium and the ionosphere induces frequency structure whose width varies as ν^3 . This effect applies only to observations made with linearly polarized antennas. However, antennas that are nominally circularly polarized are always imperfect in that they will be sensitive at some level to the position angle of a linearly polarized signal. Differential Faraday rotation over the 1.25 MHz bandwidth of our receiver amounts to only $\sim 10^{-2}$ radians for PSR 0950+08 at 430 MHz, so this effect is negligible.

b) Numerical Results

i) Single Pulses

A pulse from PSR 0950+08 is shown in Figure 1 in which micropulses and more amorphous, longer-duration features are evident. Single pulses differ markedly from the average of several hundred pulses also shown in Figure 1; some show only the amorphous structure while others are dominated by very intense micropulses, like the pulse in Figure 2a. Micropulses have a characteristic width of $\sim 200 \mu\text{s}$, although some are at least a factor of 10 narrower, like those in Figure 2a. Our goal was to study the radio-frequency spectra for blocks of data that enclose, at most, one micropulse. We therefore computed finite Fourier transforms (of the baseband signal before detection) for 256 sample blocks, corresponding to $204.8 \mu\text{s}$ of time.

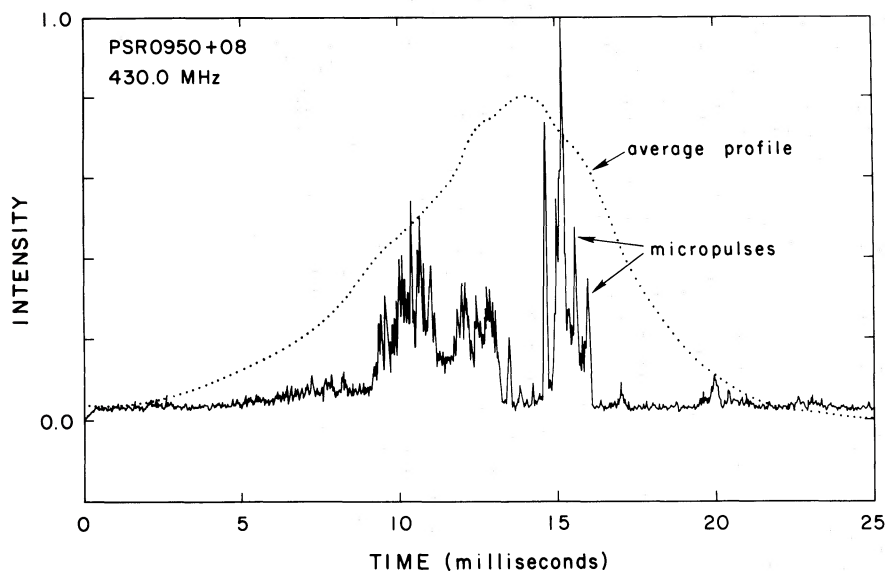


FIG. 1.—A single pulse from PSR 0950+08 with distinct micropulses as well as amorphous subpulse structure. Postdetection smoothing is $25 \mu\text{s}$. The peak flux is $\sim 625 \text{ Jy}$. The dotted line is the average of several hundred single pulses.

Blocks were spaced by 256 samples so that 128 spectra per pulse were computed, some of which nominally contained only off-pulse sky-background and receiver noise.

Spectra of the two micropulses in Figure 2a are shown in Figure 2b accompanied by spectra of off-pulse noise. Structure in the spectra is obviously stochastic, but one cannot determine by visual inspection whether the spectra conform to the amplitude-modulated noise model. Are the largest peaks in spectra A and B of Figure 2b consistent with the model? The model predicts that fluctuations in the spectrum should have widths equal to the reciprocal micropulse width. Amplitudes of the fluctuations must *on average* yield a unity value for the ratio of the standard deviation to the mean. For a single spectrum the significance of spikes can be tested by placing confidence limits on the spectrum. Confidence limits are difficult to calculate for this particular spectrum, however, so a Monte Carlo technique was used.

The peaks in the spectra of Figure 2b are roughly 7 times the mean spectral level. We computed spectra of simulated amplitude-modulated noise and found that 12% of the peak values were greater than 7 times the mean level of the spectrum. Therefore, we conclude that the amplitudes of the spectra in Figure 2b are consistent with amplitude-modulated noise.

The ACF of the spectra in Figure 2b is shown in Figure 3. Fluctuations of the ACF are within the bounds predicted by the model. The expected standard deviation of the residual ACF (on-pulse ACF minus off-pulse ACF) in Figure 3 is $\sigma(\delta\nu) \approx 0.14r_s(\delta\nu)$, where we have assumed that two micropulses with $\sim 20 \mu\text{s}$ widths yield $N_i \sim 2 \times (1.25 \text{ MHz})(20 \mu\text{s}) = 50$ independent spectral fluctuations. The $\sim 50 \text{ kHz}$ width of the spike near zero lag is also consistent with the $20 \mu\text{s}$ micropulse widths.

ii) Average Autocorrelation Function

To test the AMN model in a quantitatively precise way, we computed average autocorrelation functions by summing ACFs of individual on-pulse and off-pulse spectra of 60 pulses. The ACFs are shown in Figure 4 along with the difference of the on-pulse and the off-pulse ACFs. The on-pulse ACF has estimation errors $\sigma_r(\delta\nu) \approx 0.008r_s(\delta\nu)$ which account for all the noisiness in the residual ACF. The residual ACF has a slight negative bias of ~ -0.003 , which can be accounted for by normalization error in either the on-pulse or the off-pulse ACF. Therefore, within the statistical uncertainties, the on-pulse and the off-pulse ACFs are identical and they conform to the AMN model. The amplitude of the zero-lag spike is 0.5 ± 0.008 for the on-pulse ACF, meaning that the spectral modulation index (eq. [8]) is $m_\nu = 1.0 \pm 0.016$.

IV. DISCUSSION

a) Observational Implications

We have shown that the radiation from pulsar PSR 0950+08 is accurately described as amplitude-modulated Gaussian noise. Observationally, our results imply that there are very few unresolved (widths $\lesssim 0.8 \mu\text{s}$) micropulses and that there are no significant transient or sustained spectral lines in the signal.

Unresolved micropulses will extend over a frequency range that is larger than the receiver bandwidth, thus causing the broad portion of the ACF in equation (8) [$\propto r_H(\delta\nu)$] to be of larger amplitude than $\Delta(\delta\nu)$. The zero-lag spike therefore would have an amplitude less than 0.5, which, of course, is not observed. Hankins and Boriakoff (1978) observed very occasional unresolved micropulses in the same data analyzed here. Our results are not in disagreement with those of

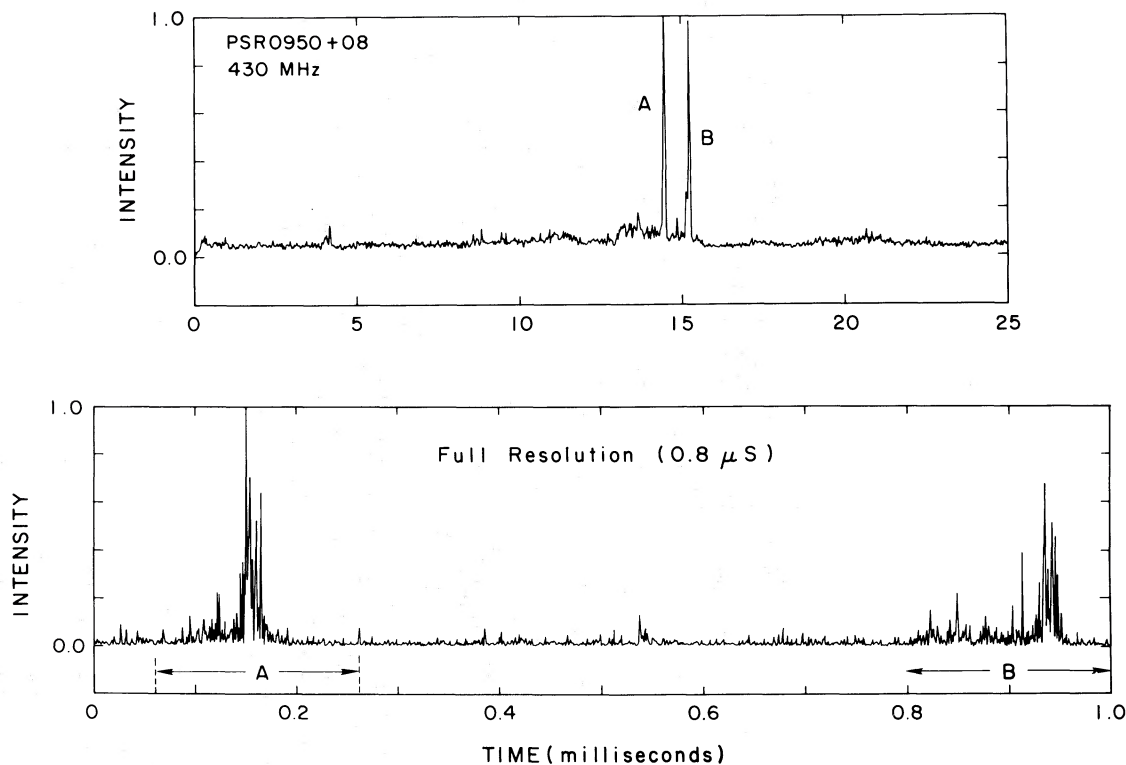


FIG. 2a

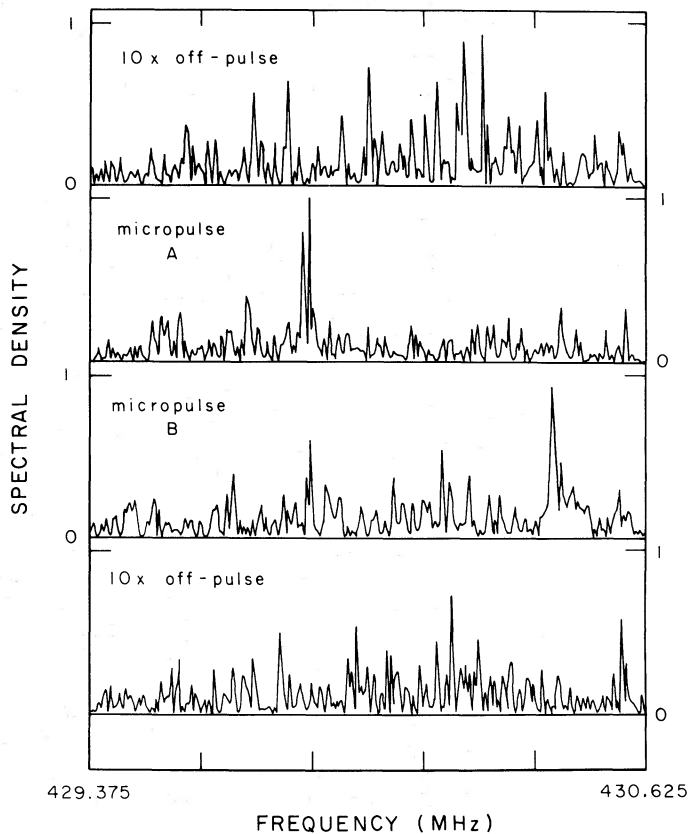


FIG. 2b

FIG. 2.—(a) A single pulse from PSR 0950+08 with two distinct micropulses. The 1 ms segment of data that contains micropulses A and B is also shown with the full $0.8 \mu\text{s}$ resolution. Micropulses have $\sim 20 \mu\text{s}$ full widths at half-intensity. The peak flux of micropulse A is $\sim 350 \text{ Jy}$ in the low-resolution plot and $\sim 850 \text{ Jy}$ in the full-resolution plot. (b) Radio frequency spectra of micropulses A and B in Fig. 2a and of off-pulse data. Frequency resolution is 5 kHz.

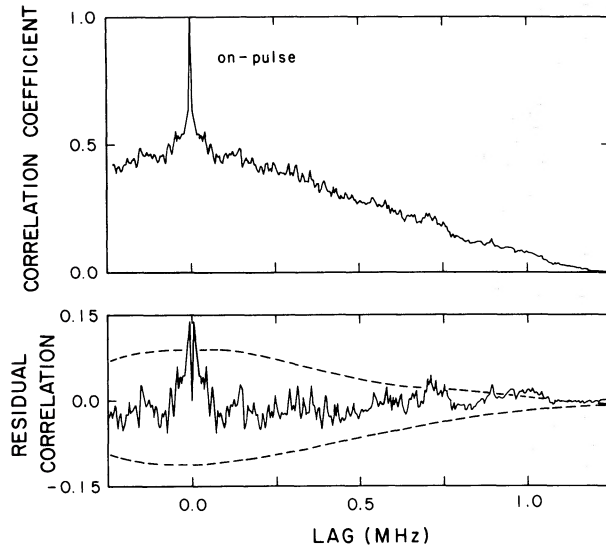


FIG. 3.—Autocorrelation function of the spectra of the two micropulses from Fig. 2. Dotted lines are the 1.5σ estimation errors of the residual ACF (the off-pulse ACF of Fig. 4 subtracted from the ACF here).

Hankins and Boriakoff because unresolved micropulses contribute negligibly to the correlation functions, owing to their infrequent occurrence.

If spectral lines or *any* perturbations from a flat spectrum exist on small frequency scales (e.g., $\lesssim 1$ MHz), then the second moment of $m(t)$ will not be exactly of the form of equation (3). The broad portion of the spectral ACF will be proportional to $r_H(\delta\nu)r_L(\delta\nu)$, where r_L is the ACF of the line shape $L(\nu)$. The presence of spectral lines would therefore cause the on-pulse ACF to have a shape different from that of the off-pulse ACF. This, also, was not observed. Our observations therefore do not substantiate those of Udal'tsov and Zlobin (1974), who reported on transient spectral lines with 1–4 MHz bandwidths and 1 minute lifetimes for PSR 0950+08 at 100 MHz.

The interpretation of Gaussian statistics encompasses a discussion of the nature of individual coherent emission regions and the manner in which they combine to form the observed signals. Studies of the time-domain statistics of pulsar signals from PSR 2016+28 (Cordes 1976a) and PSR 0950+08 (Hankins and Boriakoff 1978) indicate a large number of independent contributions in intervals as small as $0.8\ \mu\text{s}$. Similarly, the frequency domain study presented here indicates a large number of independent contributions in a frequency interval of 5 kHz. Consequently, we can infer that the number of independent fluctuations in each resolution cell of size $\Delta\nu\Delta t = (0.8\ \mu\text{s})(5\ \text{kHz})$ is a large number.

b) Coherent Emitters

What is the nature of each independent fluctuation which we suppose is the emission from a single coherent emission region? A single emitter may

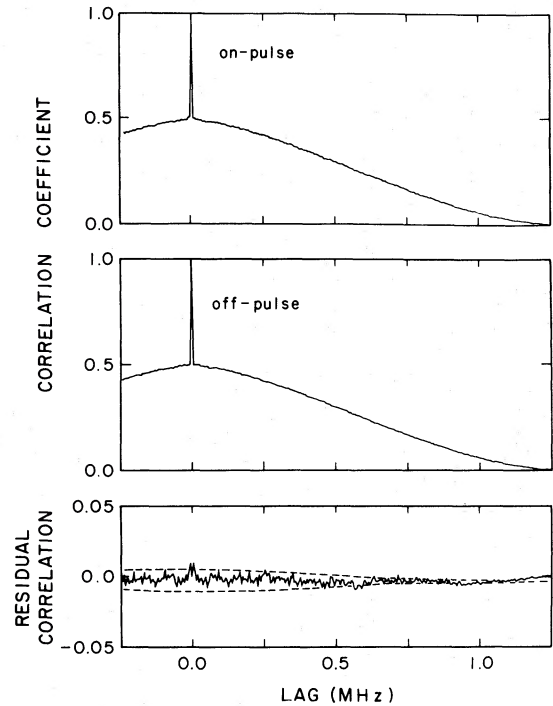


FIG. 4.—Average autocorrelation functions (ACFs) of on- and off-pulse spectra computed by summing ACFs of 1440 on-pulse spectra and 600 off-pulse spectra, respectively. The residual ACF is the difference of the on- and off-pulse ACFs. Dotted lines show the expected estimation errors ($\pm 1.5\sigma$) of the residual ACF.

produce either broad-band (e.g., bandwidth ~ 1 GHz) or narrow-band (bandwidth $\ll 1$ GHz) radiation. A coherent broad-band emitter by definition produces a very narrow (1 ns) pulse, and therefore an ensemble of emitters produces a signal that is essentially shot noise (Cordes 1976b). The signal from a narrow-band emitter is a wave packet whose time and frequency widths are related by the uncertainty principle. Consequently, our observations of micropulses with durations $\delta t \sim 200\ \mu\text{s}$ require wave-packet bandwidths $\Delta\nu \gtrsim 5\ \text{kHz}$. Individual micropulses are radiated over bandwidths at least as large as 1.25 MHz and in some instances over several hundred MHz (Rickett, Hankins, and Cordes 1975). Individual emitters need not radiate over the entire 1.25 MHz or 200 MHz range, however. What is required is that the emitter center frequency vary by several hundred MHz over an ensemble of emitters (Cordes and Rickett 1980).

Regardless of the type of emitter, we note that the time-bandwidth product of coherent emission is always of order unity. The time-bandwidth product of individual micropulses is $\gtrsim (200\ \mu\text{s})(200\ \text{MHz}) \sim 10^{4.6}$, again implying that a large number of incoherently adding emitters contribute to a micropulse. Furthermore, the physical process that causes micropulses is likely to be distinct from that which causes coherence because of the vast disparity of time scales involved: $200\ \mu\text{s}$ compared to 1–10 ns, or roughly five orders of magnitude.

Our observations are incapable of determining whether emitters are broad-band or narrow-band; we can only put a lower limit on the bandwidth of each emitter. In another paper (Cordes and Rickett 1980) we demonstrate that the only potentially observable difference between the two kinds of emitters is the presence of large peaks and valleys in the spectrum on ~ 10 – 100 MHz frequency scales for the case of narrow-band emitters. Broad-band emitters will yield spectra whose fluctuations have a modulation index (ratio of the standard deviation to the mean) of unity. The observed spectrum for narrow-band emitters is the *distribution* of emitters in frequency, which may have peaks and valleys because of a variation in radiation efficiency as a function of frequency; the modulation index will therefore be greater than unity.

c) Energy Density Calculations

Manchester *et al.* (1973) and Bartel (1978) have calculated radiation-energy densities within the context of a certain radiation model in which the micropulse bandwidth is a relevant quantity. A certain misconception exists regarding the frequency structure

discussed in this paper and by Rickett, Hankins, and Cordes (1975). The correct interpretation of the results of Rickett, Hankins, and Cordes (1975) is that micropulses from PSR 0950+08 have bandwidths of at least 200 MHz. The “deep” modulation of micropulse spectra on 5–50 kHz frequency scales is simply a consequence of Gaussian statistics that we have attributed to the noise in the AMN model. Such 5–50 kHz structure has *no* relevance to energy density calculations. Contrary to statements by Bartel (1978), the 10 MHz microstructure bandwidth assumed by Manchester *et al.* is a conservative underestimate—not an overestimate—of the micropulse bandwidth for PSR 0950+08.

We thank B. J. Rickett for useful discussions and V. Boriakoff for help in obtaining the data. The National Astronomy and Ionosphere Center is operated by Cornell University under contract with the National Science Foundation. The research was also supported by NSF grant AST 75-23581 and is contribution number 264 of the Five College Observatories.

REFERENCES

- Bartel, N. 1978, *Astr. Ap.*, **62**, 393.
 Cordes, J. M. 1976a, *Ap. J.*, **208**, 944.
 ———. 1976b, *Ap. J.*, **210**, 780.
 Cordes, J. M., and Hankins, T. H. 1977, *Ap. J.*, **218**, 484.
 Cordes, J. M., and Rickett, B. J. 1980, *Ap. J.*, submitted.
 Hankins, T. H. 1972, *Ap. J. (Letters)*, **177**, L11.
 Hankins, T. H., and Boriakoff, V. 1978, *Nature*, **276**, 45.
 Hankins, T. H., and Rickett, B. J. 1975, *Methods Comp. Phys.*, **14**, 55.
 Manchester, R. N., Tadamaru, E., Taylor, J. H., and Huguenin, G. R. 1973, *Ap. J.*, **185**, 951.
 Rickett, B. J. 1975, *Ap. J.*, **197**, 185.
 ———. 1977, *Ann. Rev. Astr. Ap.*, **15**, 479.
 Rickett, B. J., Hankins, T. H., and Cordes, J. M. 1975, *Ap. J.*, **201**, 425.
 Sutton, J. M. 1971, *M.N.R.A.S.*, **155**, 51.
 Udalt'sov, V. A., and Zlobin, V. N. 1974, *Astr. Ap.*, **37**, 21.

J. M. CORDES: Astronomy Department, Cornell University, Space Sciences Building, Ithaca, NY 14853

T. H. HANKINS: Arecibo Observatory, Post Office Box 995, Arecibo, Puerto Rico 00612